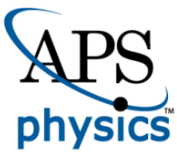

This is the accepted manuscript made available via CHORUS. The article has been published as:

Neutron Skins and Neutron Stars in the Multimessenger Era

F. J. Fattoyev, J. Piekarewicz, and C. J. Horowitz

Phys. Rev. Lett. **120**, 172702 — Published 25 April 2018

DOI: 10.1103/PhysRevLett.120.172702

Neutron skins and neutron stars in the multi-messenger era

F. J. Fattoyev,[1,*] J. Piekarewicz,[2,†] and C. J. Horowitz[1,‡]

[1] *Center for Exploration of Energy and Matter and Department of Physics, Indiana University, Bloomington, IN 47405, USA*

[2] *Department of Physics, Florida State University, Tallahassee, FL 32306, USA*

(Dated: February 13, 2018)

The historical first detection of a binary neutron star merger by the LIGO-Virgo collaboration [B. P. Abbott *et al.* Phys. Rev. Lett. 119, 161101 (2017)] is providing fundamental new insights into the astrophysical site for the r-process and on the nature of dense matter. A set of realistic models of the equation of state (EOS) that yield an accurate description of the properties of finite nuclei, support neutron stars of two solar masses, and provide a Lorentz covariant extrapolation to dense matter are used to confront its predictions against tidal polarizabilities extracted from the gravitational-wave data. Given the sensitivity of the gravitational-wave signal to the underlying EOS, limits on the tidal polarizability inferred from the observation translate into constraints on the neutron-star radius. Based on these constraints, models that predict a stiff symmetry energy, and thus large stellar radii, can be ruled out. Indeed, we deduce an upper limit on the radius of a $1.4\,M_\odot$ neutron star of $R_\star^{1.4}<13.76\,\text{km}$. Given the sensitivity of the neutron-skin thickness of ^{208}Pb to the symmetry energy, albeit at a lower density, we infer a corresponding upper limit of about $R_{\rm skin}^{208}\lesssim 0.25\,\text{fm}$. However, if the upcoming PREX-II experiment measures a significantly thicker skin, this may be evidence of a softening of the symmetry energy at high densities—likely indicative of a phase transition in the interior of neutron stars.

PACS numbers: 04.40.Dg, 21.60.Jz, 21.65.Ef, 24.10.Jv, 26.60.Kp, 97.60.Jd

What are the new states of matter at exceedingly high density and temperature? and *how were the elements from iron to uranium made?* are two of the "eleven science questions for the next century" identified by the National Academies Committee on the Physics of the Universe [1]. In framing these questions, the committee recognized the deep connections between the very small and the very large. In one clean sweep, the historical first detection of a binary neutron star (BNS) merger by the LIGO-Virgo collaboration [2] has started to answer these fundamental questions by providing critical insights into the nature of dense matter and on the synthesis of the heavy elements.

Gravitational waves (GW) from the BNS merger GW170817 emitted from a distance of about 40 Mpc were detected by the LIGO gravitational-wave observatory [2]. About two seconds later, the Fermi Gamma-ray Space Telescope (Fermi) [3] and the International Gamma-Ray Astrophysics Laboratory (INTEGRAL) [4] identified a short duration γ-ray burst associated with the BNS merger. Within eleven hours of the GW detection, ground- and spaced-based telescopes operating at a variety of wavelengths identified the associated *kilonova*—the electromagnetic transient powered by the radioactive decay of the heavy elements synthesized in the rapid neutron-capture process (r-process). Characteristics of the light curve, such as its fast rise, decay, and rapid color evolution, are consistent with the large opacity typical of the lanthanides (atomic number 57–71) and have revealed that about 0.05 solar masses (or about 10^4 earth masses) of r-process elements were synthesized in this single event [5–8]. The gravitational wave detection from the BNS merger, together with its associated electromagnetic counterparts, open the new era of *multi-messenger* astronomy and provide compelling evidence in favor of the long-held belief that neutron-star mergers play a critical role in the production of heavy elements in the cosmos.

Besides the identification of the BNS merger as a dominant site for the r-process, such an unprecedented event imposes significant constraints on the EOS of dense matter. In particular, the *tidal polarizability* (or deformability) is an intrinsic neutron-star property highly sensitive to the compactness parameter (defined as GM/c^2R) [9–14] that describes the tendency of a neutron star to develop a mass quadrupole as a response to the tidal field induced by its companion [15, 16]. The dimensionless tidal polarizability Λ is defined as follows:

$$\Lambda = \frac{2}{3}k_2\left(\frac{c^2R}{GM}\right)^5 = \frac{64}{3}k_2\left(\frac{R}{R_s}\right)^5 , \qquad (1)$$

where k_2 is the second Love number [17, 18], M and R are the neutron star mass and radius, respectively, and $R_s\equiv 2GM/c^2$ is the Schwarzschild radius. A great virtue of the tidal polarizability is its high sensitivity to the stellar radius ($\Lambda\sim R^5$) a quantity that has been notoriously difficult to constrain [19–29]. Pictorially, a "fluffy" neutron star having a large radius is much easier to polarize than the corresponding compact star with the same mass but a smaller radius. Finally, a derived quantity from the individual tidal polarizabilities Λ_1 and Λ_2 related to the phase of the gravitational wave [16, 18, 30, 31] is given

by

$$\widetilde{\Lambda}=\frac{16}{13}\left[\frac{(M_1+12M_2)M_1^4}{(M_1+M_2)^5}\Lambda_1+\frac{(M_2+12M_1)M_2^4}{(M_1+M_2)^5}\Lambda_2\right]. \quad (2)$$

Note that for the equal-mass case, $\widetilde{\Lambda}=\Lambda_1=\Lambda_2$. Remarkably, the tidal polarizability determined from the first BNS merger is already stringent enough to rule out a significant number of previously viable EOSs [2].

In this letter we explore in greater detail the impact of the BNS merger on the EOS and on those laboratory observables that are particularly sensitive to the nuclear symmetry energy—a quantity that represents the increase in the energy of the system as it departs from the symmetric limit of equal number of neutrons and protons; see Refs. [32–34] and references contained therein. Particularly uncertain is the density dependence of the symmetry energy, often encoded in a quantity denoted by L that is closely related to the pressure of pure neutron matter at saturation density.

A laboratory observable that has been identified as strongly correlated to both L and to the radius of low-mass neutron stars is the *neutron-skin thickness* of atomic nuclei—defined as the difference between the neutron (R_n) and proton (R_p) root-mean-square radii: $R_{\rm skin}=R_n-R_p$. Despite a difference in length scales of 19 orders of magnitude, the size of a neutron star and the thickness of the neutron skin share a common origin: the pressure of neutron-rich matter. That is, whether pushing against surface tension in an atomic nucleus or against gravity in a neutron star, both the neutron skin and the stellar radius are sensitive to the same EOS.

The pioneering Lead Radius Experiment (PREX) at the Jefferson Laboratory has provided the first model-independent evidence in favor of a neutron-rich skin in ^{208}Pb [35, 36]: $R_{\rm skin}^{208}=0.33^{+0.16}_{-0.18}$ fm. Although the central value is significantly larger than suggested by most theoretical predictions, the large statistically-dominated (1σ) uncertainty prevents any real tension between theory and experiment. In an effort to impose meaningful theoretical constraints, an approved follow-up experiment (PREX-II) is envisioned to reach a 0.06 fm accuracy.

To connect the tidal polarizability to nuclear observables sensitive to the density dependence of the symmetry energy [13], we model the EOS using a relativistic mean-field (RMF) approach pioneered by Serot and Walecka [37, 38] which has been continuously improved throughout the years [39–42]. The effective Lagrangian density is written exclusively in terms of conventional degrees of freedom (neutrons, protons, electrons, and muons) and includes a handful of parameters that are calibrated to provide an accurate description of finite nuclei and—critically to the description of neutron stars—a Lorentz covariant extrapolation to dense nuclear matter. Although increasingly sophisticated fitting protocols are now able to incorporate more stringent constraints from finite nuclei and neutron stars [43], the *isovector* sector of the effective Lagrangian—responsible for generating the density dependence of the symmetry energy—remains largely unconstrained. To mitigate this problem we follow a simple procedure first proposed in Ref. [41] that enables one to fine tune the value of the slope of the symmetry energy L without compromising the success of the model in reproducing well measured observables. We label the set of models generated in this manner the "FSUGold2 family".

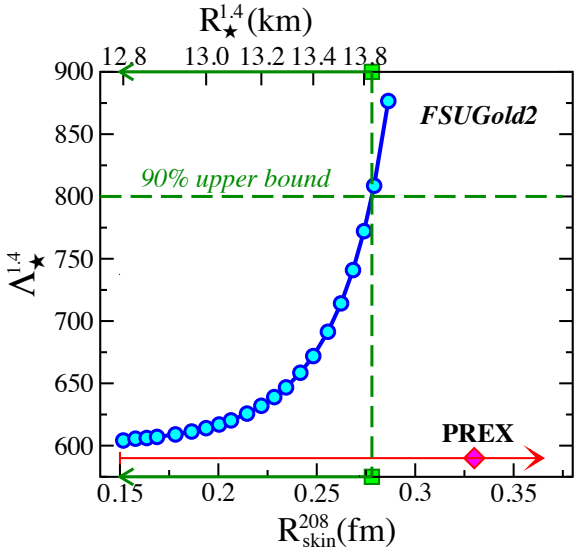

FIG. 1: (Color online). The dimensionless tidal polarizability $\Lambda_\star^{1.4}$ of a $1.4\,M_\odot$ neutron star as a function of the neutron-skin thickness of ^{208}Pb (lower abscissa) and the radius of a $1.4\,M_\odot$ neutron star (upper abscissa) as predicted by the FSUGold2 family of relativistic interactions. Constraints on $R_{\rm skin}^{208}$ and $R_\star^{1.4}$ are inferred from adopting the $\Lambda_\star^{1.4}\leq 800$ limit deduced from GW170817 [2].

In Fig. 1 we use the FSUGold2 family to predict the tidal polarizability $\Lambda_\star^{1.4}$ of a $1.4\,M_\odot$ neutron star as a function of both $R_{\rm skin}^{208}$ and $R_\star^{1.4}$ (the radius of a $1.4\,M_\odot$ neutron star). It is important to underscore that the predictions for all three observables displayed in the figure are generated from the same interaction. That is, for each member of the FSUGold2 family, the model parameters remain unchanged in going from finite nuclei to neutron stars. As anticipated, the 90% confidence limit on $\Lambda_\star^{1.4}\leq 800$ extracted from the GW signal translates into a corresponding upper limit on the radius of a $1.40\,M_\odot$ neutron star of $R_\star^{1.4}\leq 13.9$ km. Also shown in the figure is the central value of $R_{\rm skin}^{208}$ as measured by the PREX collaboration [35, 36], with the red arrow highlighting the rather large experimental uncertainty. Adopting the $\Lambda_\star^{1.4}\leq 800$ limit excludes the $R_{\rm skin}^{208}\gtrsim 0.28$ fm region—suggesting that the neutron-skin thickness of ^{208}Pb cannot be overly large. However, if the large central value of $R_{\rm skin}^{208}=0.33$ fm is confirmed by PREX-II, then an intrigu-

ing scenario may develop. A thick neutron skin would suggest that the EOS at the typical densities found in atomic nuclei is stiff, while the small neutron-star radii inferred from the BNS merger implies that the EOS at higher densities is soft. The evolution from stiff to soft may be indicative of a phase transition in the interior of neutron stars.

While the FSUGold2 family provides the flexibility to generate a continuum of realistic models with varying neutron skins, the models span a fairly narrow range of neutron-star radii (see Fig. 1). To alleviate this problem—and in the spirit of Ref. [2]—we provide predictions using a representative set of RMF models. As in the case of the FSUGold2 family, these models are successful in reproducing laboratory observables and are also consistent with the $M_\star = 2.01 \pm 0.04\, M_\odot$ limit [44, 45]. Yet, being less restrictive than the FSUGold2 family, they can generate a wider range of stellar radii. For reference, the ten models adopted in this letter are: NL3 [46, 47], IU-FSU [48], TAMUC-FSU [49], FSUGold2 [43], and FSUGarnet together with three parametrizations denoted by RMF022, RMF028, and RMF032 [50].

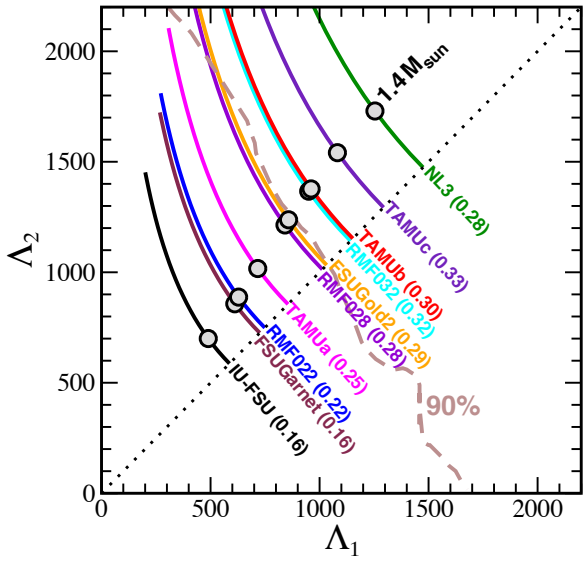

FIG. 2: (Color online). Tidal polarizabilities Λ_1 and Λ_2 associated with the high-mass M_1 and low-mass M_2 components of the binary predicted by a set of ten distinct RMF models. Models to the right side of the 90% probability contour extracted from Ref. [2] are ruled out. The solid circles represent model predictions for a BNS system having masses of $M_1 = 1.4\, M_\odot$ and $M_2 = 1.33\, M_\odot$, respectively.

In Fig. 2 we display predictions from all ten models for the individual tidal polarizabilities Λ_1 and Λ_2 associated with the high-mass M_1 and low-mass M_2 components of the binary, respectively. The individual curves are generated by allowing the high mass star to vary independently within the $1.365 \leq M_1/M_\odot \leq 1.60$ range, whereas the low mass component is determined by maintaining the chirp mass fixed at the observed value of $\mathcal{M} = (M_1 M_2)^{3/5}(M_1{+}M_2)^{-1/5} = 1.188\, M_\odot$ [2]. Given that $R^{208}_{\rm skin}$ provides a proxy for the stiffness of the symmetry energy near saturation density, we display in parentheses the corresponding predictions for all ten models. Also shown is the 90% probability contour extracted from the low-spin scenario assumed in Fig. 5 of Ref. [2]. For reference, we also highlight predictions for a binary system having a high-mass component of $M_1 = 1.4\, M_\odot$ ($M_2 = 1.33\, M_\odot$); this gives a rough indication of how rapidly each model moves away from the equal-mass case (denoted by the dotted line).

As shown in Eq. (1), the tidal polarizability is highly sensitive to the compactness of the neutron star. For a given mass, models with a stiff symmetry energy (large L) are highly effective in pushing against gravity, thereby generating large stellar radii and correspondingly large tidal polarizabilities. The 90% contour recommended by the LIGO-Virgo collaboration is stringent enough to disfavor overly stiff EOSs. Indeed, the four RMF models with the stiffest symmetry energy, shown to the right of the 90% contour in Fig. 2, are ruled out. The next two stiffest models considered here—FSUGold2 and RMF028—follow closely the 90% contour.

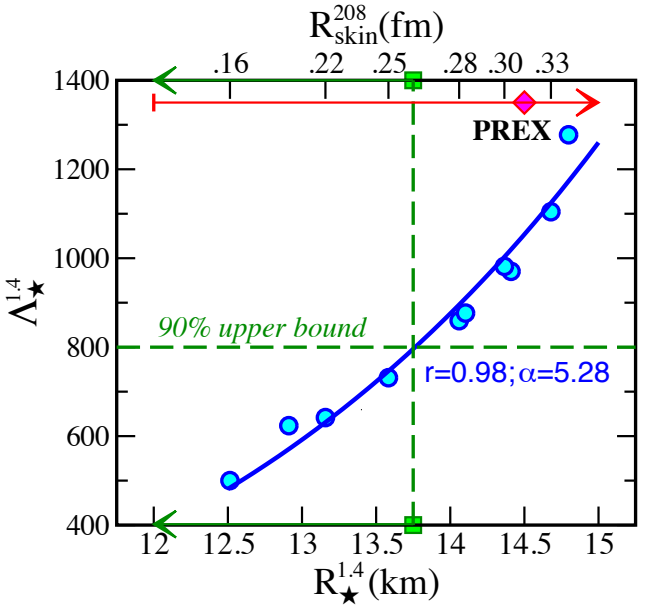

FIG. 3: (Color online). As in Fig.1, predictions are shown for $\Lambda^{1.4}_\star$ as a function of the radius of a $1.4\, M_\odot$ neutron star and the neutron-skin thickness of ^{208}Pb, but now for the ten RMF models discussed in the text.

In analogy to Fig. 1, we display in Fig. 3 the tidal polarizability of a $1.4\, M_\odot$ neutron star as a function of the corresponding stellar radius and the neutron-skin thickness of ^{208}Pb, but now for the ten selected RMF models. The solid line represents a two-parameter fit to the predictions of the ten models of the form $\Lambda_\star = a R^\alpha_\star$. We

obtain $a \approx 7.76 \times 10^{-4}$ and $\alpha \approx 5.28$, with a robust correlation coefficient of $r \approx 0.98$. Note that the exponent α is consistent with the scaling behavior suggested in Eq. (1). Also note that predictions for tidal polarizabilities, stellar radii, and neutron skins are made without ever changing the parameters of each individual model.

As already alluded in Fig. 2, limits imposed on the tidal polarizability by GW170817 rule out the four models with the stiffest symmetry energy. Now Fig. 3 illustrates how the impact of the $\Lambda_\star^{1.4} \leq 800$ limit translates into a limit on the stellar radius of a $1.4 M_\odot$ neutron star of $R_\star^{1.4} < 13.76\,\text{km}$. This is in excellent agreement with the $R_\star^{1.4} < 13.9\,\text{km}$ limit inferred previously from Fig. 1. However, the $\Lambda_\star^{1.4} \leq 800$ limit is now stringent enough to rule out all but the four models with the softest symmetry energy. Given that both L and $R_{\rm skin}^{208}$ are correlated to the radius of "low-mass" neutron stars [51], deducing limits on these two quantities from the radius of a $1.4 M_\odot$ neutron star may be model dependent. Nevertheless, using the stiffest of the models that survives the $\Lambda_\star^{1.4} \leq 800$ constraint as a guideline (*i.e.,* TAMUC-FSUa) one obtains: $R_\star^{1.4} = 13.6\,\text{km}$, $R_{\rm skin}^{208} = 0.25\,\text{fm}$, and $L = 82.5\,\text{MeV}$. It is important to note that while we have used a relatively large and representative set of relativistic mean-field models, our findings should be confronted against other theoretical approaches to test the robustness of our conclusions.

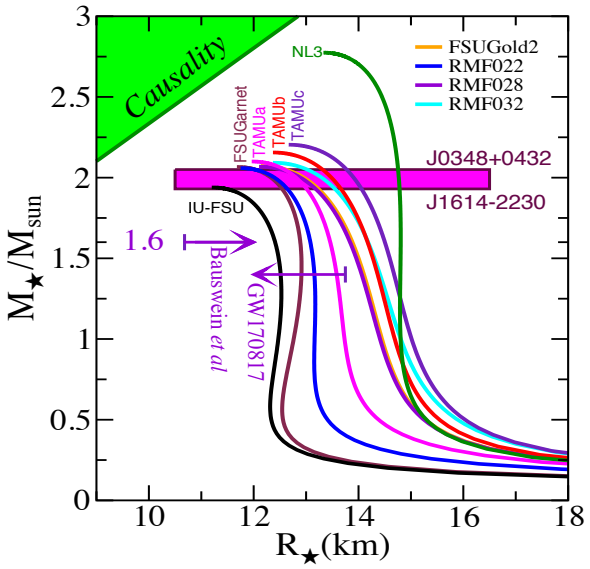

FIG. 4: (Color online). Mass-vs-Radius relation predicted by the ten RMF models discussed in the text. Mass constraints obtained from electromagnetic observations of two neutron stars are indicated with a combined uncertainty bar [44, 45]. In contrast, the arrows indicate constraints on stellar radii obtained exclusively from GW170817 and exclude many of the otherwise acceptable equations of state. The excluded causality region was adopted from Fig. 2 of Ref. [52].

We conclude by displaying in Fig. 4 the "holy-grail" of neutron-star structure: the mass-*vs*-radius (MR) relation. Note that each EOS generates a unique MR relation. Interestingly, the inverse statement is also true: exact knowledge of the MR relation uniquely determines the EOS [53, 54]. Typically, the EOS is written as a sum of two distinct contributions: (a) one for symmetric matter having equal number of neutrons and protons and (b) one for the symmetry energy to account for deviations from the symmetric limit. For RMF models of the kind described here, the maximum stellar mass is largely controlled by the high-density component of the EOS of symmetric matter. In contrast, stellar radii—as well as tidal polarizabilities—are sensitive to the symmetry energy at about twice nuclear-matter saturation density. However, stellar radii are also sensitive to the EOS of the inhomogeneous crust [52, 55, 56]. At densities relevant to the inner crust, the system exhibits rich and complex structures that emerge from a dynamical competition between short-range nuclear attraction and long-range Coulomb repulsion. Due to this complexity, at present the EOS of the inner crust is not well known. Hence, for this region we have adopted the EOS described in Ref. [57]. As already mentioned, all RMF models generate an EOS that is sufficiently stiff to support a $M_\star \approx 2\,M_\odot$ neutron star [44, 45]. In addition, Fig. 4 incorporates our newly-inferred 13.76 km upper limit on $R_\star^{1.4}$. Interestingly enough, a *lower limit* on the stellar radius of a $1.6\,M_\odot$ neutron star of $R_\star^{1.6} = 10.68^{+0.15}_{-0.04}$ was obtained by Bauswein *et al.,* under the assumption that the BNS merger did not result in a prompt collapse [58]. Finally, we use the results obtained in Fig. 3 to deduce a *lower limit* on the tidal polarizability of a $1.4\,M_\odot$ neutron star. To do so, we note that PREX imposes a lower bound on the neutron-skin thickness of ^{208}Pb of $R_{\rm skin}^{208} \simeq 0.15\,\text{fm}$, which corresponds to a stellar radius of $R_\star^{1.4} \simeq 12.55\,\text{km}$. Using the fit displayed in Fig. 3, the limit on $R_\star^{1.4}$ translates into a corresponding lower limit on the tidal polarizability of $\Lambda_\star^{1.4} \simeq 490$; see Ref. [59] for an alternative extraction of a lower bound on the tidal deformability parameter. Thus, combining observational constraints from the LIGO-Virgo collaboration with laboratory constraints from the PREX collaboration, the tidal polarizability of a $1.4\,M_\odot$ neutron star falls within the following range of values: $490 \lesssim \Lambda_\star^{1.4} \lesssim 800$.

In summary, we have examined how the historical first detection of gravitational waves from the merger of two neutron stars improves our knowledge of the EOS of dense matter. While the BNS merger provides fundamental insights on the site of the r-process and confirms its association to short γ-ray burst, our aim in this letter was to illuminate its connection to laboratory observables. Such a connection is possible because of the sensitivity of the tidal polarizability to the stellar radius, which probes the symmetry energy at about twice nuclear-matter saturation density. Assuming that one can extrapolate down to saturation density, constraints

from GW170817 provide limits on the neutron-skin thickness of ^{208}Pb—a fundamental laboratory observable that is strongly correlated to the slope of the symmetry energy at saturation density. Indeed, by exploring the consequences of the $\Lambda_\star^{1.4} \leq 800$ limit provided by the LIGO-Virgo collaboration, we deduced a limit on the stellar radius of a $1.4\,M_\odot$ neutron star of $R_\star^{1.4} < 13.76\,\mathrm{km}$. In turn, this translates into a neutron-skin thickness of ^{208}Pb of $R_{\rm skin}^{208} \lesssim 0.25\,\mathrm{fm}$, which is well below the upper limit obtained by the PREX collaboration. Conversely, by relying on PREX lower limit on $R_{\rm skin}^{208}$, we were able to provide a lower limit on the tidal polarizability of $\Lambda_\star^{1.4} \gtrsim 490$. Finally, given that the PREX experiment reported a central value of $R_{\rm skin}^{208} \lesssim 0.33\,\mathrm{fm}$—albeit with large error bars—an intriguing possibility emerges. If the follow-up experiment PREX-II confirms that $R_{\rm skin}^{208}$ is large, this will suggest that the EOS at the typical densities found in atomic nuclei is stiff. In contrast, the relatively small neutron-star radii suggested by GW170817 implies that the symmetry energy at higher densities is soft. The evolution from stiff to soft may be indicative of a phase transition in the neutron-star interior. Undoubtedly, the multi-messenger era is in its infancy and much work remains to be done. Yet, it is remarkable that the very first observation of a BNS merger already provides a treasure trove of insights into the nature of dense matter.

We are grateful to Katerina Chatziioannou and Jocelyn Read for clarifying the LIGO-Virgo results presented in Ref. [2]. This material is based upon work supported by the U.S. Department of Energy Office of Science, Office of Nuclear Physics under Awards DE-FG02-87ER40365 (Indiana University), Number DE-FG02-92ER40750 (Florida State University), and Number DE-SC0008808 (NUCLEI SciDAC Collaboration).

* Electronic address: ffattoye@indiana.edu
† Electronic address: jpiekarewicz@fsu.edu
‡ Electronic address: horowit@indiana.edu

[1] *Connecting Quarks with the Cosmos: Eleven Science Questions for the New Century* (The National Academies Press, Washington, 2003).
[2] B. P. Abbott et al. (Virgo, LIGO Scientific), Phys. Rev. Lett. **119**, 161101 (2017).
[3] A. Goldstein et al., Astrophys. J. **848**, L14 (2017).
[4] V. Savchenko et al., Astrophys. J. **848**, L15 (2017).
[5] M. R. Drout et al., Science **358**, 1570 (2017).
[6] P. S. Cowperthwaite et al., Astrophys. J. **848**, L17 (2017).
[7] R. Chornock et al., Astrophys. J. **848**, L19 (2017).
[8] M. Nicholl et al., Astrophys. J. **848**, L18 (2017).
[9] T. Hinderer, Astrophys. J. **677**, 1216 (2008).
[10] T. Hinderer, B. D. Lackey, R. N. Lang, and J. S. Read, Phys. Rev. **D81**, 123016 (2010).
[11] T. Damour and A. Nagar, Phys. Rev. **D80**, 084035 (2009).
[12] S. Postnikov, M. Prakash, and J. M. Lattimer, Phys. Rev. **D82**, 024016 (2010).
[13] F. J. Fattoyev, J. Carvajal, W. G. Newton, and B.-A. Li, Phys. Rev. **C87**, 015806 (2013).
[14] A. W. Steiner, S. Gandolfi, F. J. Fattoyev, and W. G. Newton, Phys. Rev. **C91**, 015804 (2015).
[15] T. Damour, M. Soffel, and C. Xu, Phys. Rev. **D45**, 1017 (1992).
[16] E. E. Flanagan and T. Hinderer, Phys. Rev. **D77**, 021502 (2008).
[17] T. Binnington and E. Poisson, Phys. Rev. **D80**, 084018 (2009).
[18] T. Damour, A. Nagar, and L. Villain, Phys. Rev. **D85**, 123007 (2012).
[19] F. Ozel, G. Baym, and T. Guver, Phys. Rev. **D82**, 101301 (2010).
[20] A. W. Steiner, J. M. Lattimer, and E. F. Brown, Astrophys. J. **722**, 33 (2010).
[21] V. Suleimanov, J. Poutanen, M. Revnivtsev, and K. Werner, Astrophys. J. **742**, 122 (2011).
[22] S. Guillot, M. Servillat, N. A. Webb, and R. E. Ruledge, Astrophys.J. **772**, 7 (2013).
[23] J. M. Lattimer and A. W. Steiner, Astrophys. J. **784**, 123 (2014).
[24] C. O. Heinke, H. N. Cohn, P. M. Lugger, N. A. Webb, W. Ho, et al., Mon. Not. Roy. Astron. Soc. **444**, 443 (2014).
[25] S. Guillot and R. E. Rutledge, Astrophys.J. **796**, L3 (2014).
[26] F. Ozel, D. Psaltis, T. Guver, G. Baym, C. Heinke, and S. Guillot, Astrophys. J. **820**, 28 (2016).
[27] A. L. Watts et al., Rev. Mod. Phys. **88**, 021001 (2016).
[28] A. W. Steiner, C. O. Heinke, S. Bogdanov, C. Li, W. C. G. Ho, A. Bahramian, and S. Han (2017), arXiv:1709.05013.
[29] J. Nattila, M. C. Miller, A. W. Steiner, J. J. E. Kajava, V. F. Suleimanov, and J. Poutanen, Astron. Astrophys. **608**, A31 (2017).
[30] T. Damour and A. Nagar, Phys. Rev. **D81**, 084016 (2010).
[31] L. Baiotti, T. Damour, B. Giacomazzo, A. Nagar, and L. Rezzolla, Phys. Rev. Lett. **105**, 261101 (2010).
[32] M. Tsang, J. Stone, F. Camera, P. Danielewicz, S. Gandolfi, et al., Phys.Rev. **C86**, 015803 (2012).
[33] B.-A. Li, A. Ramos, G. Verde, and I. Vidaña, Eur. Phys. J. A **50** (2014).
[34] C. J. Horowitz, E. F. Brown, Y. Kim, W. G. Lynch, R. Michaels, et al., J. Phys. **G41**, 093001 (2014).
[35] S. Abrahamyan, Z. Ahmed, H. Albataineh, K. Aniol, D. S. Armstrong, et al., Phys. Rev. Lett. **108**, 112502 (2012).
[36] C. J. Horowitz, Z. Ahmed, C. M. Jen, A. Rakhman, P. A. Souder, et al., Phys. Rev. **C85**, 032501 (2012).
[37] J. D. Walecka, Annals Phys. **83**, 491 (1974).
[38] B. D. Serot and J. D. Walecka, Adv. Nucl. Phys. **16**, 1 (1986).
[39] J. Boguta and A. R. Bodmer, Nucl. Phys. **A292**, 413 (1977).
[40] H. Mueller and B. D. Serot, Nucl. Phys. **A606**, 508 (1996).
[41] C. J. Horowitz and J. Piekarewicz, Phys. Rev. Lett. **86**, 5647 (2001).
[42] B. G. Todd-Rutel and J. Piekarewicz, Phys. Rev. Lett **95**, 122501 (2005).
[43] W.-C. Chen and J. Piekarewicz, Phys. Rev. **C90**, 044305

(2014).
[44] P. Demorest, T. Pennucci, S. Ransom, M. Roberts, and J. Hessels, Nature **467**, 1081 (2010).
[45] J. Antoniadis, P. C. Freire, N. Wex, T. M. Tauris, R. S. Lynch, et al., Science **340**, 6131 (2013).
[46] G. A. Lalazissis, J. Konig, and P. Ring, Phys. Rev. **C55**, 540 (1997).
[47] G. A. Lalazissis, S. Raman, and P. Ring, At. Data Nucl. Data Tables **71**, 1 (1999).
[48] F. J. Fattoyev, C. J. Horowitz, J. Piekarewicz, and G. Shen, Phys. Rev. **C82**, 055803 (2010).
[49] F. J. Fattoyev and J. Piekarewicz, Phys. Rev. Lett. **111**, 162501 (2013).
[50] W.-C. Chen and J. Piekarewicz, Phys. Lett. **B748**, 284 (2015).
[51] J. Carriere, C. J. Horowitz, and J. Piekarewicz, Astrophys. J. **593**, 463 (2003).
[52] J. M. Lattimer and M. Prakash, Phys. Rept. **442**, 109 (2007).
[53] L. Lindblom, Astrophys. J. **398**, 569 (1992).
[54] W.-C. Chen and J. Piekarewicz, Phys. Rev. Lett. **115**, 161101 (2015).
[55] J. Piekarewicz, F. J. Fattoyev, and C. J. Horowitz, Phys. Rev. **C90**, 015803 (2014).
[56] M. Fortin, C. Providencia, A. R. Raduta, F. Gulminelli, J. L. Zdunik, P. Haensel, and M. Bejger, Phys. Rev. **C94**, 035804 (2016), 1604.01944.
[57] J. W. Negele and D. Vautherin, Nucl. Phys. **A207**, 298 (1973).
[58] A. Bauswein, O. Just, N. Stergioulas, and H.-T. Janka (2017), 1710.06843.
[59] D. Radice, A. Perego, and F. Zappa (2017), 1711.03647.